

Fourier transform infrared investigation of thin perfluoropolyether films exposed to electric fields

F.E. Spada^a and D. Basov^b

^a Center for Magnetic Recording Research, University of California, San Diego, La Jolla, CA 92093-0401, USA

^b Department of Physics, University of California, San Diego, La Jolla, CA 92093-0319, USA

Received 21 April 2000; accepted 1 May 2000

Reflection–absorption Fourier transform infrared (FTIR) techniques were used to monitor thin layers of hydroxyl-terminated perfluoropolyether lubricant (Fomblin ZDOL) for molecular changes caused by long exposures to dc electric fields with intensities in the range $3\text{--}6 \times 10^4$ V/cm. A new absorption band appears in the $1720\text{--}1640$ cm^{-1} region of some field-exposed specimens. The new spectral feature is attributed to the presence of C=O, a functional group not present in the ZDOL chemical structure but commonly found in perfluoropolyether degradation products. The peak position of the carbonyl absorption band indicates that hydrogenated carbon is present at the α -position. The presence of hydrogenated α -carbons suggests that structural modifications occur via a mechanism that primarily involves the $-\text{CH}_2\text{--OH}$ functional endgroup, rather than the more commonly proposed bond cleavage at the $-\text{O--CF}_2\text{--O-}$ acetal groups in perfluoropolyether lubricants having no polar endgroups. These results suggest that slow but cumulative lubricant degradation may occur when strong electric fields are present at the head–disk interface.

Keywords: FTIR, lubricant degradation, perfluoropolyethers, ZDOL, tribology, electric fields, disk drives

1. Introduction

Perfluoropolyethers (PFPE) are widely used as surface lubricants on magnetic media in disk drives, and play a critical role in protecting both the carbon overcoat and the underlying magnetic layer from damage caused by slider–disk contacts during normal operation. Because the lubricant layer on the disk surface is extremely thin ($5\text{--}20$ Å), lubricant stability is an important factor that directly influences the long-term reliability of disk drives [1]. It is now well-known that PFPE lubricants can degrade via chemical incompatibility with materials at the interface [2–8], elevated temperatures [4,8–12], mechanical shearing [13], and electron-induced damage [2,7,10,12,14–18]. Consideration of the situation at the slider–disk interface suggests that electron-mediated mechanisms should play a more prominent role in PFPE degradation as fly heights decrease. This is because the increased frequency of slider–disk contacts will enhance the opportunities for surface charging or “triboelectric” events such as those proposed earlier [2,7,14,17]. Another reason is that modest potential differences at the head–disk interface are capable of producing electric field intensities E in the range $10^4\text{--}10^6$ V/cm, as reported for earlier drive products [19]. With today’s fly heights near 200 Å, potentials as small as 0.1 V would produce a field intensity of about 5×10^4 V/cm. Field strengths of this magnitude may be capable of initiating molecular processes leading to lubricant breakdown. In fact, recent reports indicate that streamer inception, partial discharge and breakdown can occur in a variety of PFPE fluids at field strengths as low as $E \approx 2 \times 10^4$ V/cm [20–22]. Also noteworthy is the fact that present day and projected

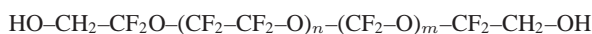
future fly heights are less than the length of the magnetoresistive sensor, as well as the thicknesses of the insulating layers separating the sensor from the shields and pole tips in the recording head. This situation increases the possibility for small electrical leakage currents to flow between disk and sensor during normal operation if the dielectric strength of the head–disk interface drops below that of the insulating layers.

It is generally accepted that electrical breakdown cannot occur across the head–disk interface because the mean free path of an electron in air at normal temperature and pressure (~ 1000 Å) far exceeds current flying heights. This situation does not provide for a sufficient number of electron–molecule ionizing encounters required for the charge amplification needed to initiate spark discharge in the gap. The importance of charge amplification can be observed in plots of breakdown voltage V_b as a function of the product pd , where p is pressure and d is electrode separation. For gaps larger than a few microns V_b exhibits a minimum in these plots. This is referred to as Paschen behavior [23] and reflects how the probability of ionization varies with the number of gas molecules in the gap, a quantity proportional to pd . The minimum value of V_b is about 300 V for air [23,24], which is two to three orders of magnitude greater than typical voltages at the head–disk interface and, therefore, consistent with the assumption that breakdown should not pose a serious reliability problem. Furthermore, as with electrostatic discharge (ESD) events [25], breakdown would produce high current density discharges (limited only by the capacity of the external circuit), collapse of the potential difference across the gap, locally elevated temperatures, and damage to the electrode surfaces. These

occurrences would be obvious as well as catastrophic for the interface, but no reports have yet appeared in the open literature which implicate electrical breakdown as a significant interface problem in operating disk drive products.

It is important, however, to distinguish between complete breakdown and the *prebreakdown* events leading to discharge. The importance of prebreakdown ionization currents has roots in studies dating back to the early 1900's which show that Paschen behavior is *not* observed for vacuum and air microgaps [23,24,26–29]. For these very small gaps V_b appears to be proportional to d , and breakdown occurs at gap potentials of the order of a few volts (ac and dc). It has been suggested that this behavior arises from very intense local fields at projections on the gap surfaces which produce cold field electron emission, followed by complete breakdown when a conductive plasma forms at the asperity tip [23,24,28–30]. However, studies attempting to account for asperities have repeatedly shown that prebreakdown currents appear at field intensities substantially lower than predicted by the Fowler–Nordheim theory describing cold field emission, and that the derived asperity dimensions are often physically unrealistic [23,28,29,31]. Thus, electron emission in microgaps must occur via a mechanism not fully described by theory. Examination of the recent literature indicates that the exact nature of gaseous and vacuum prebreakdown processes is still a topic of considerable interest [31,32]. In contrast to complete breakdown and ESD discharges, prebreakdown events are characterized by very low current densities which have little influence on the gap voltage, negligible temperature excursions, and no damage to the electrode surfaces. Consequently, the signatures of prebreakdown events may not be obvious. Such events nevertheless may be capable of initiating electron-induced reaction processes requiring prolonged periods before PFPE degradation becomes detectable. It is reasonable, therefore, to consider the possibility that the very small currents caused by intense electric fields at the head–disk interface may contribute to lubricant failure even in the absence of complete breakdown.

In this paper we use Fourier transform infrared (FTIR) spectroscopy to explore whether static dc electric fields can affect the stability of the hydroxyl-terminated Fomblin variety of PFPE lubricant (trade name ZDOL) having chemical structure



ZDOL was chosen because of its widespread use in disk drives. A capacitor model was employed for our experiments, in which thin PFPE layers deposited on the capacitor plate surfaces were subjected to an electric field within a small air gap separating the plates. The capacitor model was selected because of its simplicity, and the fact that its stationary nature eliminated potentially interfering influences from elevated temperatures and shearing forces always present at rubbing interfaces during conventional tribological studies of lubricant stability. Reflection absorption FTIR methods were chosen because changes in

the lubricant layer could be monitored directly without the need for sampling techniques that can alter molecular structure (e.g., fragmentation–ionization for NMR analysis, and X-ray irradiation for XPS analysis).

2. Experimental

Samples for these studies consisted of ZDOL layers on thin Au films sputtered onto standard microscope slides. The Au layers served both as the conductive capacitor plates as well as reflective layers for the reflection–absorption FTIR measurements. Au is also known to be chemically compatible with PFPE lubricants over a large temperature range [4]. Prior to deposition of the Au layer, the glass substrates were soaked in a hot concentrated KOH solution for about 3 h, rinsed several times with distilled water and dried at 150 °C overnight to remove any traces of dimethyl silicone lubricant, a common surface contaminant on commercial microscope slide surfaces [33]. Immediately after cooling, the substrates were placed in the sputtering chamber and pumped to 5×10^{-7} Torr background pressure. A 100 Å Ni adhesion layer and a 1000 Å Au layer were dc sputtered at 2 mTorr Ar pressure during the same pump-down. Deposition rates were 12 Å/min for the Ni underlayer and 100 Å/min for the Au layer.

Substrates were coated with Fomblin lubricants by dip coating from 10 mg/ml solutions of lubricant in either FC113 (1,1,2-trichlorotrifluoroethane, Fisher) or Vertrel (1,1,1,2,3,4,4,5,5,5-decafluoropentane, DuPont) solvents. Fomblin ZDOL (2000 MW) and ZDIAC (2000 MW) lubricants were used. The latter is a dicarboxylic-acid-terminated PFPE and served as a reference material, as described later. All solvents and lubricants were used as-received from the vendor without further purification or drying, and lubricants were not fractionated to improve their molecular weight distribution prior to use. The dip procedure consisted of a 1 min soak time and a 1 mm/s withdrawal rate in ambient laboratory air. A Candela optical surface analyzer was used to measure lubricant thicknesses on smaller substrates (1000 Å Au/100 Å Ni on Si) prepared in the same manner. ZDOL layer thicknesses on these smaller specimens were in the range ~100–110 Å and were considered representative of lubricant thicknesses on the larger glass substrates. This thickness was chosen to improve sensitivity to small changes in the FTIR spectra. Specimens were stored in separate polypropylene individual wafer shipping trays (Fluoroware) to avoid cross-contamination of surfaces after dip coating.

The “capacitor” test cell consisted of two ZDOL-coated substrates with 45 mm × 25 mm overlapping electrode areas placed face-to-face against an approximately 5 μm thick polytetrafluoroethylene (PTFE, Goodfellow) gasket having a 39 mm × 19 mm rectangular air gap. This assembly was rigidly mounted in a solid PTFE block with a 25 g load on the top electrode to press the specimen surfaces against the PTFE gasket. The cell was placed in an electrically

Table 1
Summary of experimental details for field-exposed ZDOL-coated specimens.

Experiment	Change in FTIR spectra	d_{meas} (μm)	E (10^4 V/cm)	Exposure (h)	i^a (A)	Q^b (C)
F1 ^c	Yes	29.8	3.4	88	$(0.2\text{--}1.3) \times 10^{-5}$	0.63–4.2
F2 ^c	No	20.1	5.0	117	$(0.002\text{--}0.5) \times 10^{-9}$	$8 \times 10^{-7}\text{--}2.1 \times 10^{-4}$
F3 ^c	No	19.2	5.2	109	$(0.002\text{--}2) \times 10^{-6}$	0.0008–0.8
V1 ^d	Yes	18.3	5.5	292	$(0.04\text{--}0.8) \times 10^{-5}$	0.42–8.4
V2 ^d	No	22.6	4.4	115	$(0.002\text{--}1.0) \times 10^{-5}$	0.01–4.1

^a Minimum and maximum currents recorded during field exposure.

^b Tabulated values represent estimated total transferred charge during field exposure, based on duration of field exposure and the observed minimum/maximum currents. Values are not based on current integration.

^c ZDOL layers on both anode and cathode. ZDOL coatings prepared from solutions of ZDOL in FC113 solvent.

^d ZDOL layer on anode, bare Au cathode. ZDOL coatings prepared from solutions of ZDOL in Vertrel solvent.

grounded solid aluminum Faraday shield to provide a dark and noise-free environment. Electrical contact to the Au film surfaces was made via copper clips attached to the end of a triaxial cable. Effective separations between the electrode surfaces were determined from capacitance measurements made with a Solartron 1260 impedance analyzer (1 kHz, 0.1 V rms applied voltage). In order to account for the dielectric contribution of the PTFE gasket, the test cell was assumed to be composed of two parallel capacitors with identical electrode separation d , one filled with only air and having area S_{air} of the rectangular air gap, and the other filled with PTFE of thickness $t_{\text{PTFE}} < d$ (balance of the gap separation filled with air) and having area S_{PTFE} of the PTFE gasket surface. The cell capacitance C was therefore expressed as

$$C = \frac{\varepsilon_0 \varepsilon_{\text{air}} S_{\text{air}}}{d} + \frac{\varepsilon_0 \varepsilon_{\text{air}} S_{\text{PTFE}}}{d - [(\varepsilon_{\text{PTFE}} - 1)t_{\text{PTFE}}/\varepsilon_{\text{PTFE}}]}, \quad (1)$$

where $\varepsilon_0 = 8.85 \times 10^{-14}$ F/cm, $\varepsilon_{\text{air}} = 1$, and $\varepsilon_{\text{PTFE}} = 2.1$ are the permittivity of free space, the dielectric constant for air, and the dielectric constant for PTFE, respectively. The value $t_{\text{PTFE}} = 4.1 \mu\text{m}$ was determined from weights of several large specimens of PTFE gasket material having known area, and the density of PTFE (2.2 g/cm^3). Effective electrode separations (d_{meas}) determined from equation (1) were found to be in the range $16 \mu\text{m} < d_{\text{meas}} < 30 \mu\text{m}$. Neglecting the presence of the PTFE gasket would have reduced the d_{meas} values by about 4%.

A Hewlett–Packard 4140 B picoammeter/voltage source was used to supply voltage to the cell and measure current i . The dc voltage across the cell was increased from 0 to 100 V in 1–10 V steps and i recorded after each step. The cell potential was then maintained at 100 V for varying periods, producing macroscopic electric field intensities of about $3\text{--}6 \times 10^4$ V/cm and within the range previously reported at the head–disk interface [19]. A current-limiting circuit prevented i from exceeding 10^{-4} A at all times. Current integration was not performed during these experiments, but rough estimates of the total transferred charge Q were obtained from the current magnitudes and durations of field exposure. All field exposures were conducted in air at 23 °C. The details of several field-exposure experiments are summarized in table 1.

Some important details regarding the experimental setup should be noted. The time constant of the picoammeter circuit was several tens to hundreds of milliseconds during these experiments. Because the primary intent of this study was to investigate the influence of field-induced small currents on PFPE stability and not to monitor the details of breakdown processes, no attempts were made to resolve faster electrical events. Cell impedance phase angles were $\theta = -89.6 \pm 0.3^\circ$ and, using a parallel RC equivalent circuit model, cell resistances were always $>10 \text{ M}\Omega$ and cell capacitances were in the range $3\text{--}6 \times 10^{-10}$ F. Measured capacitances did not vary with dc bias potentials up to 41 V, the upper bias voltage limit of the impedance analyzer, and it was therefore assumed that d_{meas} did not change with cell voltage. As noted above, the d_{meas} values derived from capacitance measurements were several times greater than the thickness of the PTFE gasket, but consistent with the 15–20 μm variation in substrate flatness inferred from the white light interference pattern produced by random pairs of glass substrates when placed on top of one another. The electric field between the electrodes was therefore not ideally uniform, and quoted values for E refer to macroscopic intensities based on d_{meas} . Breakdown or shorting across projections on opposing surfaces was sometimes observed and could be deliberately induced with loads greater than 25 g on the top electrode. Such events could be recognized by triggering of the current-limiting circuit, immediate collapse of gap voltage, and visible damage to the soft Au layer when viewed at $\times 100$ magnification.

Changes in the lubricant structure were monitored in the 4000–500 cm^{-1} spectral range with a Bruker IFS66/v FTIR single beam spectrometer having a liquid-nitrogen cooled MCT detector, a SpectraTech model 500 variable angle specular reflectance attachment, a globar source and p -polarized light. 40 mm \times 15 mm specimen areas were analyzed at 82° incident angle. Background measurements were made with Au-coated substrates having no lubricant layer. All FTIR spectra were obtained under vacuum to eliminate absorption bands from CO_2 and water vapor. Spectra are presented in their raw forms without smoothing, although background corrections were performed in some instances to correct for sloping baselines. Spectral resolutions are indicated in the figure captions.

3. Results

Figure 1 compares the initial i - V characteristics of test cells using bare and ZDOL-coated electrodes. The responses of two different cells consisting of bare Au electrodes, one with a PTFE gasket having an air gap ($d_{\text{meas}} = 16.7 \mu\text{m}$, $39 \text{ mm} \times 19 \text{ mm}$ area) and another with a solid $4.1 \mu\text{m}$ thick PTFE spacer ($d_{\text{meas}} = 18.0 \mu\text{m}$), show that the presence of the air gap causes the cell current to increase by about two orders of magnitude above the leakage value for the electrodes separated by the PTFE sheet ($\leq 10^{-10}$ A). Collapse of gap voltage and electrode damage were not observed during these measurements, indicating that breakdown or shorting had not occurred. Similar experiments with ZDOL-coated electrodes usually resulted in substantially greater currents which were more unstable over time, as also shown in figure 1. Reproducibility of the initial i - V behavior among different runs was very poor with lubricant-coated electrodes. When cell voltages were maintained at 100 V for long periods during these latter experiments, currents typically fluctuated by one to two orders of magnitude over time for any given run and by several orders of magnitude among the different runs. Subsequent microscopic examination of the electrode surfaces again revealed no evidence of damage to the ZDOL-coated electrodes, suggesting that breakdown had not occurred.

Figure 2 compares FTIR spectra of as-coated and field-exposed ZDOL layers. Following field exposure, the spectra of both electrodes from experiment F1 (table 1) have new broad absorption bands centered near 1720 – 1700 cm^{-1} , 1470 – 1450 cm^{-1} , and increased absorption near 1400 – 1380 cm^{-1} . Figure 3 shows the FTIR results obtained after field exposure during experiment V1, in which the test cell consisted of a bare cathode and ZDOL-coated anode. The spectrum of the ZDOL-coated anode (figure 3(a)) shows a broad new absorption band at $\sim 1640 \text{ cm}^{-1}$. Figure 3(b) shows that a small amount of lubricant is present on the surface of the originally bare cathode, and that the lubricant spectrum includes new broad absorption bands centered at 1700 and 1390 cm^{-1} . There were no significant changes in the intensity and position of the C–F stretching absorption near 1290 cm^{-1} following the field exposures, indicating that no substantial loss of PFPE from the electrode surfaces had occurred.

Sources of contamination that could account for the new spectral features in figures 2 and 3 could not be identified. Any contaminant originally present in either the ZDOL fluid or dip-coating solvents would have been evident in the spectra of unexposed as well as field-exposed specimens because both were prepared from the same dip-coating solutions (no differences were observed between specimens prepared with FC113 and Vertrel solvents). Also, no evidence of external contamination was observed in the spectra of field-exposed bare Au electrodes. Hydrocarbon contamination can be ruled out because the characteristic strong absorption due to C–H stretching is absent from the

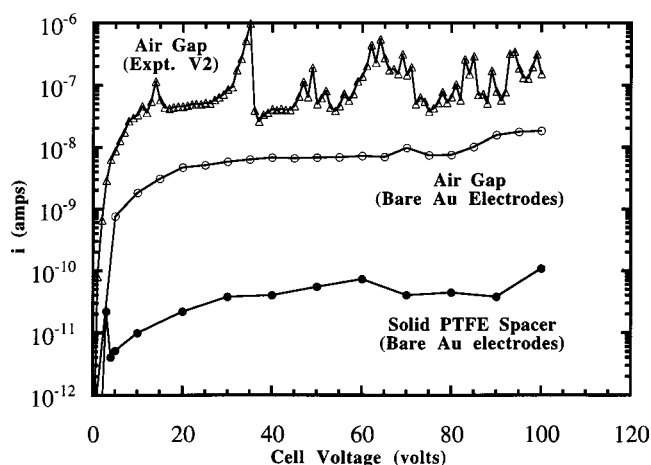


Figure 1. Initial i - V responses of test cells with bare Au electrodes separated by an air gap ($d_{\text{meas}} = 16.7 \mu\text{m}$), bare Au electrodes separated by a solid PTFE spacer ($d_{\text{meas}} = 18.0 \mu\text{m}$), and a ZDOL-coated anode and a bare Au cathode separated by an air gap (experiment V2, table 1).

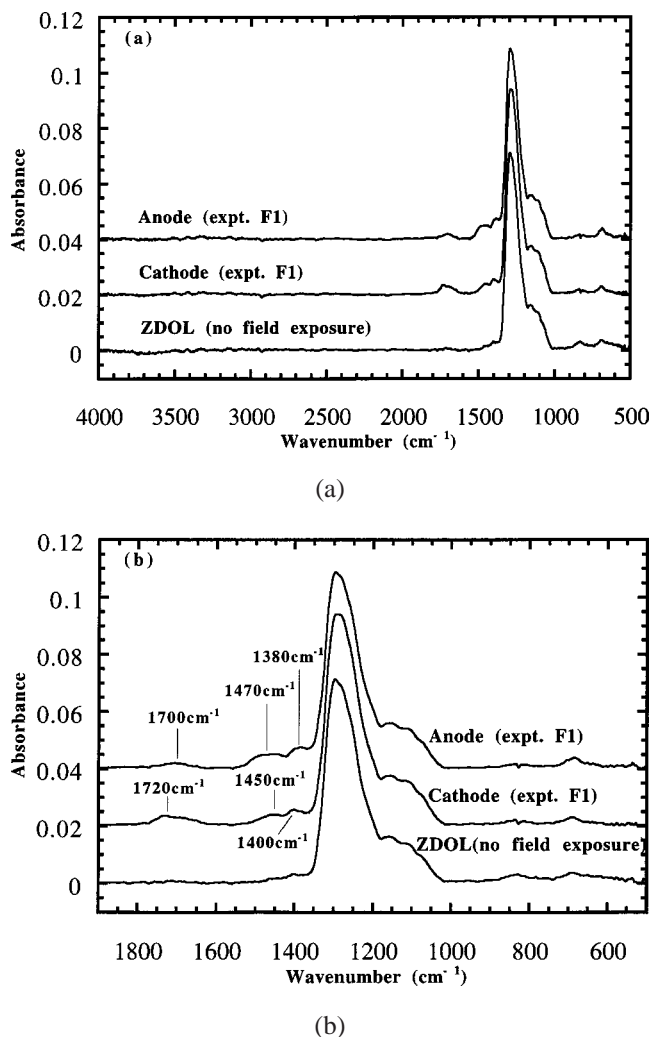


Figure 2. FTIR spectra of as-coated and field-exposed 100 \AA ZDOL specimens. Field-exposed specimens are those of experiment F1 (table 1). Spectra were obtained with 4 cm^{-1} resolution and are offset vertically for clarity. (a) 4000 – 500 cm^{-1} region, (b) expanded view of 1900 – 500 cm^{-1} region.

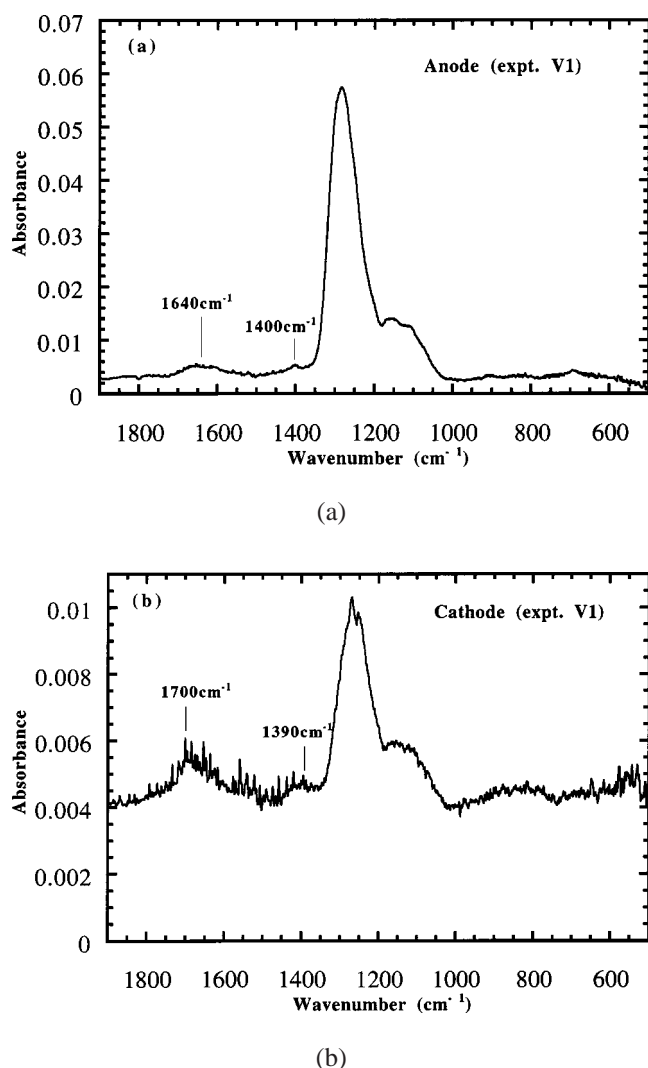


Figure 3. FTIR spectra of anode and cathode surfaces following field exposure in experiment V1 (table 1). Both spectra were obtained with 2 cm^{-1} resolution: (a) anode with 100 \AA ZDOL layer, (b) originally bare cathode.

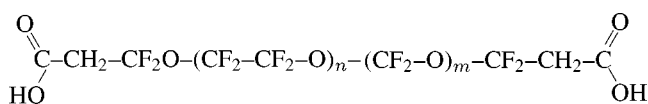
$2950\text{--}2850\text{ cm}^{-1}$ region. Although absorption in the $1680\text{--}1600\text{ cm}^{-1}$ region can arise from the O–H deformation vibration of water, moisture contamination would have also produced a much stronger O–H stretching absorption near $3300\text{--}3000\text{ cm}^{-1}$. Adsorbed water on specimen surfaces as well as icing of the MCT detector can therefore also be eliminated as possibilities.

Field exposure did not always produce significant changes in the ZDOL spectrum. The data in table 1 suggest that new absorption bands in the FTIR spectra appear only in those experiments having large values of Q . Experiment V2 appears to be an exception, but the tabulated values for Q are subject to errors arising from the large variations of i with time and represent only rough estimates of the possible ranges for the total amount of transferred charge during field exposure. Further experiments will be required to verify the correlation between Q and changes in the ZDOL spectrum.

4. Discussion

One of the commonly reported signatures of PFPE lubricant degradation is the presence of the carbonyl group (C=O) [2,3,5–9,12,13,17], which has a characteristic absorption band for the stretching vibration in the $1850\text{--}1550\text{ cm}^{-1}$ region [34,35]. The broad weak absorption bands near $1720\text{--}1640\text{ cm}^{-1}$ in figures 2 and 3 suggest that field-exposed PFPE layers contain this group, and this possibility will be the focus of the following discussion. The precise position of the carbonyl peak depends on both the nature of adjacent chemical groups and the physical state of the specimen. In degraded PFPE, C=O is usually attributed to the fluoroformate ($-\text{CF}_2\text{O-CFO}$), acyl fluoride ($-\text{CFO}$), or carboxylic acid ($-\text{COOH}$) functionalities [2,3,5,13]. But carbonyl absorption in fluoroformate and acyl fluoride typically occurs near $1900\text{--}1850\text{ cm}^{-1}$ [34,35], well above where the new bands appear in figures 2 and 3. Even if fluoroformate or acyl fluoride had formed during field exposure, both would have immediately transformed to the carboxylic acid or acetate forms in the presence of air or moisture. But reference tables [34,35] and spectra [36] show that carbonyl absorption in carboxylic acids and acetates with partially or fully fluorinated carbons at the α -position occurs in the range $1800\text{--}1710\text{ cm}^{-1}$, also higher than the position of the new bands in figures 2 and 3 (e.g., see spectra of fluoro- and trifluoroacetic acids, pentadecafluorooctanoic acid, trifluoroacetic anhydride, methyl- and ethyltrifluoroacetates [36]). Portions of the new absorption bands do extend to $\sim 1720\text{ cm}^{-1}$ but the peak positions and significant fractions of the peak areas lie at much lower wavenumber, so carbonyl with fluorinated α -carbon neighbors cannot entirely account for the chemical environment in field-exposed ZDOL specimens.

Comparisons with the FTIR spectrum of ZDIAC were used to assist with the interpretation of the field-exposed ZDOL spectra. ZDIAC is a useful reference material because it is structurally similar to ZDOL, but contains carboxylic acid groups instead of hydroxyl groups at both ends of the polymer chain:



In contrast to the molecular environments considered above, ZDIAC also contains hydrogenated carbons at the α -position, a feature which would shift the carbonyl absorption to lower wavenumber [34,35]. The FTIR spectra of 100 \AA layers of ZDOL and ZDIAC on Au (neither exposed to field) are compared in figure 4(a). The most prominent difference between the two is the peak centered at 1685 cm^{-1} in the ZDIAC spectrum. The appearance of the ZDIAC carbonyl absorption band below the $1750\text{--}1710\text{ cm}^{-1}$ range for unassociated carbonyl indicates that the C=O bond strength is weakened. This may be a consequence of the layer structure found in PFPE films thicker than a few monolayers, which consist of a thin bonded

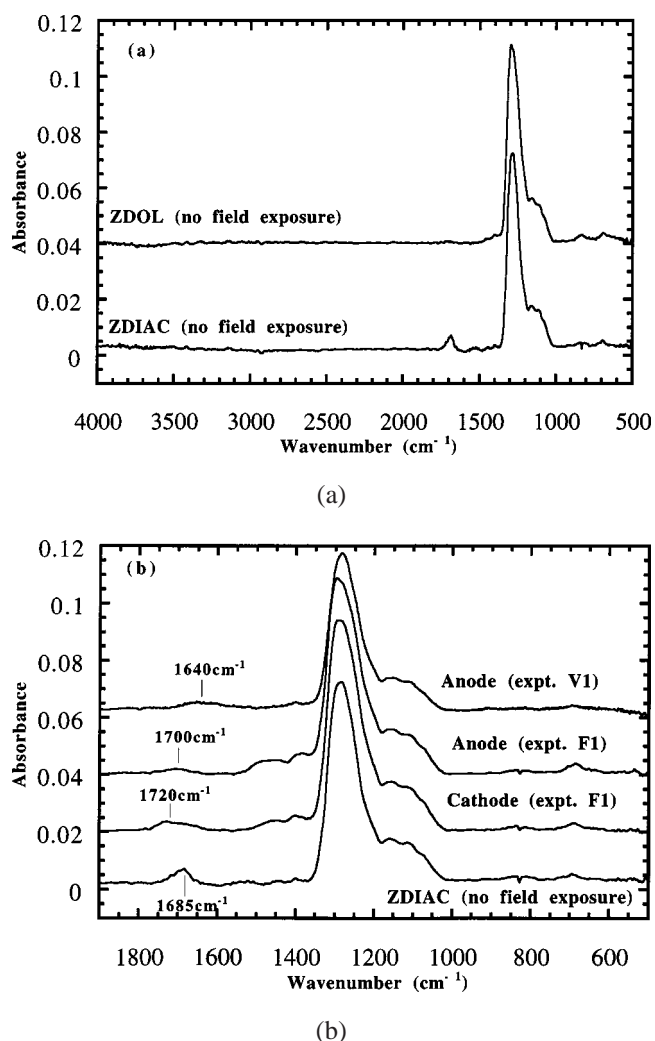
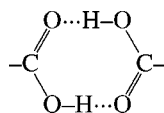
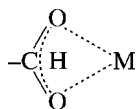


Figure 4. FTIR spectra of 100 Å ZDOL and 100 Å ZDIAC layers. Spectra are offset vertically for clarity; (a) comparison of unexposed ZDOL (4 cm^{-1} resolution) and unexposed ZDIAC layers (2 cm^{-1} resolution) over the entire 4000–500 cm^{-1} region; (b) comparison of as-coated ZDIAC layer (2 cm^{-1} resolution) with field-exposed ZDOL layers of experiments F1 (4 cm^{-1} resolution) and V1 (2 cm^{-1} resolution).

layer immediately adjacent to the substrate surface and a thicker disordered layer above it [37,38]. Intermolecular interactions such as the



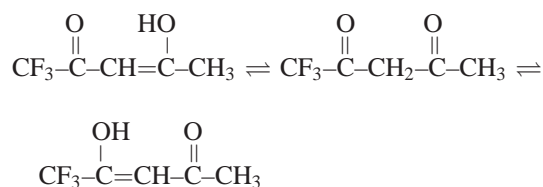
dicarboxylic acid association in the disordered layer, and



associations (M = metallic surface) in the thin bonded layer would diminish the C=O bond strength in ZDIAC and shift the C=O stretching absorption to substantially lower wavenumber [34,35,39,40]. The presence of the hydrogenated α -carbons also contributes to the shift to

lower wavenumber, as noted previously. More noteworthy, however, is the low wavenumber range in which both the ZDIAC carbonyl absorption band and the new absorption bands in the field-exposed ZDOL specimens appear (figure 4(b)), suggesting that carbonyl and carboxylic acid groups with hydrogenated α -carbon neighbors are present in field-exposed specimens.

Other plausible carbonyl-containing molecular environments can also account for the new features in the field-exposed ZDOL spectra. For example, reference tables and spectra show that in diketone structures the C=O absorption occurs in the 1700–1600 cm^{-1} region. An example is 1,1,1-trifluoro-2,4-pentanedione [36], which exhibits carbonyl absorption near 1610 cm^{-1} with a broad shoulder extending to ~ 1700 cm^{-1} . As with the case of dicarboxylic acid association noted above, this may be a consequence of the weakened C=O oscillator strength due to the presence of keto-enol transformations:



The C=C bond stretching vibration also gives rise to absorption in the 1660–1580 cm^{-1} region when conjugated with C=O, as in the enol forms above, or in the 1650–1645 cm^{-1} region if the $\text{CH}_2=\text{CF}$ functionality is present. It is interesting that the spectrum of this pentanedione also exhibits weak absorptions near 1470, 1422 and 1370 cm^{-1} characteristic of the C–O–H and C–H deformation vibrations. The spectra of field-exposed ZDOL specimens shown in figure 2 exhibit increased intensities near these positions, and suggest the possible presence of structural units with environments similar to those of the pentanedione.

Assignment of the C=O stretching vibration to the new absorption bands in the spectra of field-exposed specimens therefore appears to be quite reasonable, assuming the presence of hydrogenated carbons at the α -position and strong inter- or intramolecular interactions. The presence of carbonyl with hydrogenated α -carbons implies that the field-induced decomposition proceeds via a mechanism that primarily acts on the hydroxyl endgroups of ZDOL, without substantial effect on the $-\text{O}-\text{CF}_2-\text{O}-$ acetal groups in the polymer backbone. This is because scission of the acetal groups (often referred to as the “unzipping” mechanism and used to describe decomposition of PFPE molecules without functional endgroups [2,13,21]) would have produced a substantial fraction of products with fluorinated α -carbons. The unzipping process would have also resulted in lubricant depletion from the electrode surfaces due to the volatility of the low molecular weight products, but the invariance of the C–F stretching peak intensity near 1290 cm^{-1} indicates negligible PFPE loss occurred during field exposure.

It is unlikely that the changes in the FTIR spectra observed in this work resulted from Joule heating, even if elec-

tric currents had been localized at small lubricant bridges connecting the electrode surfaces. This can be seen by considering the case where electrical conduction is limited to a single 200 Å thick lubricant contact having 1 μm² cross-sectional area. Neglecting radiation to the surrounding air gap and considering only contact to both electrode surfaces, the maximum temperature T_{\max} at the center of the bridge can be computed from equation (2), which is valid for one-dimensional thermal conduction in a plane wall when thermal energy is being generated from electrical energy [41]

$$T_{\max} = \frac{PL^2}{2Vk} + T_s. \quad (2)$$

In this equation P is the electrical power dissipated in bridge volume V , L is the distance between the center of the bridge and the electrode surface, k is the thermal conductivity of the bridge material, and T_s is the substrate temperature. Since power dissipation across the gap was at most $\sim 10^{-3}$ W with the largest observed current in these experiments, the computed temperature rise ($T_{\max} - T_s$) of such a bridge would be 36 °C, assuming $k_{\text{PFPE}} = 7 \times 10^{-4}$ W/cm °C for the PFPE thermal conductivity [21]. Both the mass and thermal conductivity of the electrodes are several orders of magnitude greater than the corresponding quantities for the ZDOL bridge ($k_{\text{Au}} = 3.15$ and $k_{\text{glass}} \approx 8.4 \times 10^{-3} - 1.1 \times 10^{-2}$, in W/cm °C), so it is reasonable to assume that T_s remained at room temperature during these experiments. The temperature at the center of the bridge is therefore well below the 150–200 °C required for the onset of thermal degradation in bulk PFPE fluids when in contact with suitable catalysts [3,8,9,12], as well as the 300 °C intrinsic decomposition temperature of the PFPE backbone [8,9,12]. Degradation therefore must have been initiated by some electron-mediated mechanism. The tentative correlation between the appearance of new absorption bands and large Q values (table 1) is consistent with this conclusion, since the extent of electron-mediated reactions should scale with the amount of transferred charge.

The influence of environmental species on the field-induced PFPE degradation process is unknown at this time because all field exposures were conducted in ambient air, but it is quite plausible that molecular oxygen and water do play important roles. For example, ozone (O₃) and superoxide (O₂⁻) ions formed by the intense electric field within the gap could be key reactants in the degradation process since both are known to react readily with organic materials. In the presence of moisture both would form peroxides, which are also powerful reactants. Studies are currently underway to understand the role of oxygen and moisture.

The nature of the conduction process in these experiments is also unknown. Possibilities include electron emission caused by locally high fields at very small gaps between asperities, and electrolysis currents passing through lubricant bridges connecting asperities on opposing electrode surfaces or spanning the surface of the PTFE spacer. As noted above, very low concentrations of reactive species

created in the air gap could be involved in the former case, whereas direct electron transfer between lubricant and electrode would occur in the latter. The small amount of lubricant observed on the originally bare cathode of experiment V1 (figure 3(b)) suggests that some form of lubricant bridge did indeed form. Lubricant transfer between electrode surfaces may simply have arisen from PFPE migration at areas of contact, but dielectrophoretic forces could also have played a role. When subjected to *nonuniform* electric fields, such as those produced at asperities on the electrode surfaces, dielectric materials having a larger dielectric constant (e.g., PFPE) than their surrounding environment (e.g., air) move towards regions of higher field strength. Such a process may be yet another factor which contributes to lubricant buildup at the trailing edges of sliders [42], where the electric field between head and disk is most intense.

5. Summary

Thin ZDOL layers exposed to 3–6 × 10⁴ V/cm dc electric fields for long periods exhibit a new broad absorption band in the 1720–1640 cm⁻¹ region of the reflection-absorption FTIR spectrum of the lubricant layer. The new spectral feature is attributed to the presence of C=O, a structural group not present in the ZDOL chemical structure but commonly found in PFPE degradation products. The peak position of the C=O absorption band is consistent with the presence of hydrogenated α-carbon neighbors. This implies that field-induced degradation primarily affects the functional endgroup, rather than the acetal units in the PFPE polymer backbone. Because a stationary interface was used in these experiments, elevated temperatures from frictional heating and molecular scission from shearing forces can be eliminated as contributing factors. Changes in the ZDOL molecular structure were therefore caused by an electron-mediated process induced by electric fields in the air gap or fluid bridges. These results suggest that slow but cumulative lubricant degradation may occur when strong electric fields are present at the head-disk interface.

Acknowledgement

The authors wish to thank Vijay Prabhakaran for performing the Optical Surface Analyzer thickness measurements. This work was supported in part by NSF grant CMS-9632351.

References

- [1] C.M. Mate, Tribol. Lett. 4 (1998) 119.
- [2] S. Mori and W. Morales, Wear 132 (1989) 111.
- [3] P.H. Kasai, W.T. Tang and P. Wheeler, Appl. Surf. Sci. 51 (1991) 201.
- [4] P.C. Herrera-Fierro, J.W.R. Jones and S.V. Pepper, J. Vac. Sci. Technol. A 11 (1993) 354.
- [5] P. Li, E. Lyth, D. Munro and L.M. Ng, Tribol. Lett. 4 (1998) 109.

- [6] J.M. Meyers, R.M. Desrosiers, L. Cornaglia and A.J. Gellman, *Tribol. Lett.* 4 (1998) 67.
- [7] J. Wei, W. Fong, D.B. Bogey and C.S. Bhatia, *Tribol. Lett.* 5 (1998) 203.
- [8] P.H. Kasai, *J. Inform. Stor. Proc. Syst.* 1 (1999) 23.
- [9] W.R. Jones, Jr., K.J.L. Paciorek, T.I. Ito and R.H. Kratzer, *Ind. Eng. Chem. Prod. Res. Dev.* 22 (1983) 166.
- [10] G. Vurens, R. Zehring and D. Saperstein, in: *Surface Science Investigations in Tribology*, Vol. 485, eds. Y-W. Chung, A.M. Homola and G.B. Street (American Chemical Society, Washington, DC, 1992) ch. 10.
- [11] G.H. Vurens and C.M. Mate, *Appl. Surf. Sci.* 59 (1992) 281.
- [12] J.-L. Lin, C.S. Bhatia and J.T. Yates, Jr., *J. Vac. Sci. Technol. A* 13 (1995) 163.
- [13] T.E. Karis, V.J. Novotny and R.D. Johnson, *J. Appl. Polym. Sci.* 50 (1993) 1357.
- [14] B.D. Strom, D.B. Bogy, R.G. Walmsley, J. Brandt and C.S. Bhatia, *Wear* 168 (1993) 31.
- [15] G.H. Vurens, C.S. Gudeman, L.J. Lin and J.S. Foster, *IEEE Trans. Magn.* 29 (1993) 282.
- [16] S. Matsunuma, T. Miura and H. Kataoka, *Tribol. Trans.* 39 (1996) 380.
- [17] S. Matsunuma, *Wear* 213 (1997) 112.
- [18] S. Matsunuma and Y. Hosoe, *Tribol. Int.* 30 (1997) 121.
- [19] V.J. Novotny and T.E. Karis, *Adv. Inform. Stor. Syst.* 2 (1991) 137.
- [20] M. Pompili, C. Mazzetti and E.O. Forster, *Eur. Trans. Electr. Power Eng.* 4 (1994) 163.
- [21] M. Pompili, A. Mundula, C. Mazzetti and C. Puliti, in: *Proc. 4th Int. Conf. Prop. Appl. Dielectric Mater.*, Brisbane, 1994 (IEEE) p. 168.
- [22] H. Yamashita, M. Okumura, K. Yamazawa, C. Pompili, C. Mazzetti and E.O. Forster, in: *Proc. 4th Int. Conf. Prop. Appl. Dielectric Mater.*, Brisbane, 1994 (IEEE) p. 610.
- [23] F. Llewellyn-Jones, *Ionization and Breakdown in Gases* (Methuen, London, 1957).
- [24] I.S. Taev and V.N. Kuznetsov, *Elektrotehnika* 7 (1975) 54.
- [25] A.J. Wallash, T.S. Hughbanks and S.H. Voldman, *J. Electrostatics* 38 (1996) 159.
- [26] G.M. Hobbs, *Philos. Mag. J. Sci.* 10 (1905) 617.
- [27] C. Kinsley, *Philos. Mag. J. Sci.*, 9 (1905) 692.
- [28] F. Llewellyn-Jones, *Ionization Avalanches and Breakdown* (Methuen, London, 1967).
- [29] F. Llewellyn-Jones, in: *The Advanced Study Institute on Breakdown and Discharges in Gases*, 1981, Les Arcs (Plenum, New York, 1983) p. 1.
- [30] F. Llewellyn-Jones, in: *4th Int. Conf. Gas Discharges*, 1976 (Institute of Electrical and Electronic Engineers, UK and Republic of Ireland Section) p. 429.
- [31] R.J. Noer, *Appl. Phys. A* 28 (1982) 1.
- [32] W.T. Diamond, *J. Vac. Sci. Technol. A* 16 (1998) 707.
- [33] P.B. Coleman, *Practical Sampling Techniques for Infrared Analysis* (CRC Press, Boca Raton, 1993).
- [34] N.P.G. Roeges, *A Guide to the Complete Interpretation of Infrared Spectra of Organic Structures* (Wiley, Chichester, 1994).
- [35] G. Socrates, *Infrared Characteristic Group Frequencies, Tables and Charts* (Wiley, Chichester, 1994).
- [36] *Merck FT-IR Atlas* (VCH, Weinheim, 1988).
- [37] V.J. Novotny, I. Hussla, J.-M. Turlet and M.R. Philpot, *J. Chem. Phys.* 90 (1989) 5861.
- [38] J. Ruhe, G. Blackman, V.J. Novotny, T. Clarke, G.B. Street and S. Kuan, *J. Appl. Polym. Sci.* 53 (1994) 825.
- [39] N.L. Alpert, W.E. Keiser and H.A. Szymanski, *IR-Theory and Practice of Infrared Spectroscopy* (Plenum, New York, 1970).
- [40] L.J. Bellamy, *The Infrared Spectra of Complex Molecules* (Chapman and Hall, London, 1980).
- [41] J.P. Holman, *Heat Transfer*, 7th Ed. (McGraw-Hill, New York, 1990) p. 38.
- [42] R.F. Wolter, V. Raman, D. Jen and D. Gillis, *J. Inf. Stor. Proc. Syst.* 1 (1999) 33.